Journal of Power Sources, 6 (1981) 171 - 184

TESTING THE MECHANICAL CHARACTERISTICS OF SINTERED NICKEL BATTERY PLAQUE AND THEIR RELATIONSHIP TO NICKEL ELECTRODE PERFORMANCE

D. H. FRITTS

Aero Propulsion Laboratory, Wright-Patterson Air Force Base, Ohio (U.S.A.)

(Received in revised form July 22, 1980)

Summary

The performance of nickel battery electrodes was investigated in respect of sintered nickel plaque mechanical characteristics. It was found that plaque fatigue, sensitivity, and hardness directly affect nickel electrode performance. In addition, wide variations in these parameters was found in various manufactured plaques. It is concluded that quality control procedures should include testing for fatigue and hardness. Recommended procedures for performing these tests are presented.

Introduction

Historically, there has been little interest in the mechanical characteristics of sintered battery electrode substrate materials. These substrates have been characterized primarily in terms of their chemical compatibility, porosity, current carrying capability, and surface area [1, 2]. They have commonly been viewed as immobile and inert "containers" for the chemically active electrode material. Recently, attention has been given to the fatigue characteristics of the plaque [3] as fatique has been shown to result in long term capacity degradation of nickel electrodes [4].

In this paper, the fatigue mechanism is further quantified by continuous *in situ* measurements of plaque growth. These growth characteristics have been mechanically simulated on a fatigue testing machine. This machine has shown that there is a marked difference in the fatigue characteristics of various plaque material.

Another important parameter that has been investigated here is plaque "hardness". It has been found that the hardness affects the short term capacity retention characteristics and the utilization efficiency of nickel electrodes. The "harder" the plaque, the poorer the performance of the electrode. The implication of this statement is quite important as it implies that the electrochemical process occurring is not independent of the substrate mechanical characteristics.

A plaque hardness testing technique has been devised which is similar to the common Brinell and Rockwell hardness tests.

Nickel electrode growth measurements

The concept that plaque fatigue is a failure mechanism implies that the plaque is cyclicly strained at a level that will cause mechanical failure of the sinter joints. In a previous work [4], it was implicitly concluded that such motion was occurring. Here, direct measurements of the strain are presented.

To measure the strain, a ferrite core from an LVDT (Linear Voltage Displacement Transducer) was suspended from the nickel electrode and its motion sensed with a differential transformer (Fig. 1). The electrode was constrained from curling by fitting it loosely in a slot with the top rigidly attached to the cell case. The electrodes tested were prepared from gridless plaque manufactured at this laboratory. The reason for eliminating the grid was to ensure that the plaque had homogeneous mechanical characteristics. Thus, strains measured in one dimension are characteristic of those in the other dimensions.

The electrodes were impregnated by the Pickett Process [5] using a 50% ETOH solution with 9% $Co(NO_3)_2$ at a pH of 3.5 and a temperature of

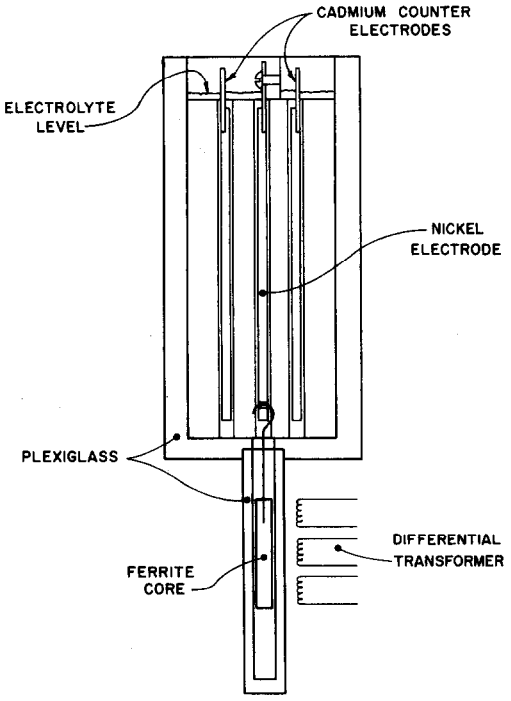

Fig. 1. Schematic of electrode growth test cell.

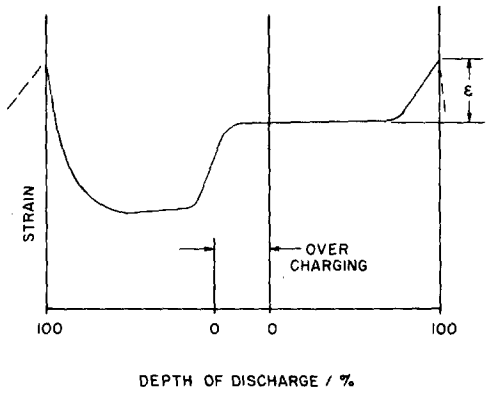

Fig. 2. Characteristic strain (growth) of nickel electrode at 1.25C rate.

80 °C. The active material loading levels were determined after three formation cycles.

The electrodes were cycled continuously from 100% depth of discharge (0.4 V cutoff) to 25% overcharge (based on a one electron exchange). The electrodes were cycled until performance (utilization efficiency) stabilized. The cycling was done at the C rate. In Fig. 2, a characteristic strain *vs.* depth of discharge curve is shown. Certain characteristics were common to all the electrodes tested, these are:

(1) the initial part of the discharge shows no growth;

(2) the subsequent growth on discharge is linear;

(3) on charge, the electrode shrinks rapidly (exponentially) and stabilizes by 60% depth of discharge;

(4) the electrode grows on overcharge, but the way a given electrode grows depends on its history. It is more sensitive to overcharge during initial cycling.

The strain that is most characteristic of an electrode is that which occurs during discharge. This is because the strain (designated by ϵ) is not overcharge sensitive. In Figs. 3 - 5, ϵ is plotted *vs.* the A h/cc of void volume obtained during discharge.

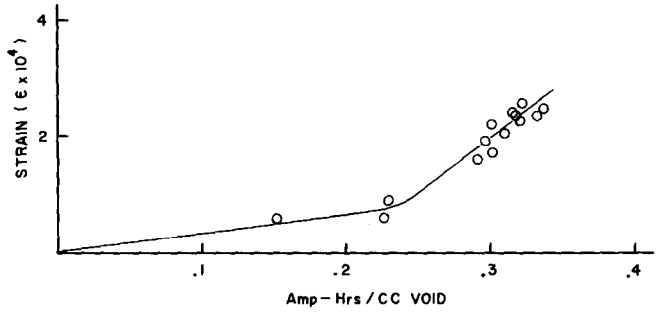

Fig. 3. Strain on discharge *vs.* A h removed per cc of void volume for a nickel plaque with a hardness of 22.50.

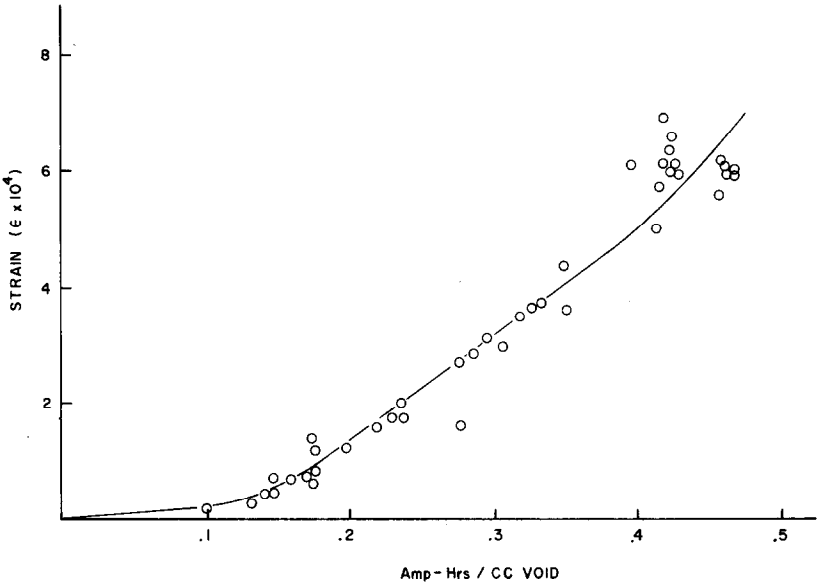

Fig. 4. Strain on discharge *vs.* A h removed per cc of void volume for a nickel plaque with a hardness of 31.25.

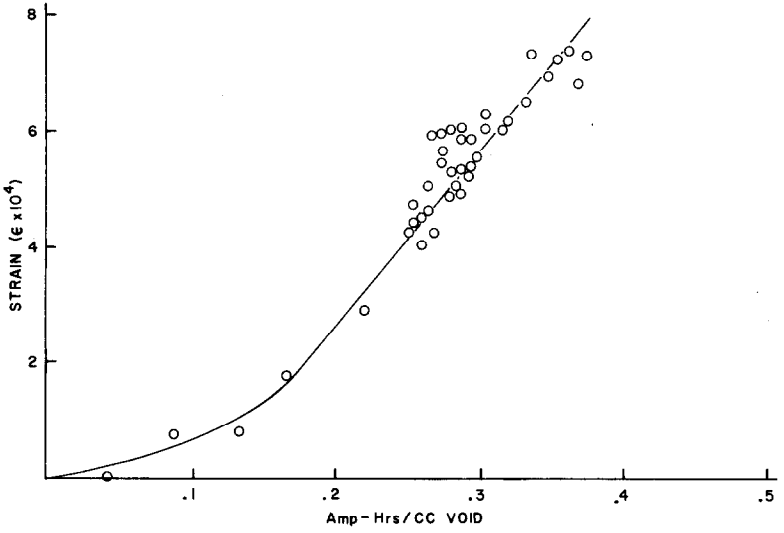

Fig. 5. Strain on discharge *vs.* A h removed per cc of void volume for a nickel plaque with a hardness of 34.84.

Each of the above Figures represents electrodes taken from the same plaque sample. The plaque samples were made in three separate furnace firings. The porosity of all the plaques was 83%, their physical appearance and dimensions were identical. The only parameter by which the plaques

could be distinguished was "hardness" (these were gridless plaques and fatique tests were not possible). The H number on these figures is a hardness indicator, with a higher H meaning a harder plaque. Details of the hardness test will be presented later. What is important, is that the harder plaque is subjected to higher strains for the same number of amp-hours of discharge. The maximum strain observed is about 10^{-3} mm/mm. Thus, in a fatigue testing device, the plaque should be subjected to strains of the same magnitude to simulate realistically the cycling strains.

Another consideration in a fatigue test is the initial prestrain that occurs during the impregnation process. In Table 1 the prestrain is shown for the impregnated plaque.

TABLE 1

Prestrain due to active material loading

Sample no.	Loading (g/cc void)	Prestrain
1	0.48	5×10^{-4}
2	0.93	3.3×10^{-3}
3	1.05	3.3×10^{-4}
4	1.20	1.0×10^{-3}
5	1.45	3.3×10^{-3}

Fatigue testing of plaque

In ref. 3, fatigue testing of plaque was done using a cyclic bending test. This method was shown to give meaningful results in correlating plaque degradation with capacity loss [4]. Unfortunately, the method has the major disadvantage that the location of the current collector grid within the plaque must be precisely known. This made it necessary to select appropriate test samples instead of using random samples. For this reason, it was decided to fatigue the plaque in tension. The tension method has two advantages: (1) insensitivity to grid location, and (2) the ability to prestrain the plaque. A cam drive, rocking beam fatigue testing machine with multiple test strain capability was designed and built. The machine is shown in Fig. 6.

The deterioration of the plaque, as it is cycled in the machine, is monitored by its increasing resistance which is due to the fatiguing and failure of the sinter bonds. All the plaque tested up to the present time had a nominal thickness of 0.75 mm, and were made to the same specifications by a single manufacturer.

In Fig. 7, two characteristic resistance *vs.* cycle curves are shown. The plaque with the larger resistance increase has poor fatigue characteristics, while the other sample has excellent fatigue characteristics. The samples

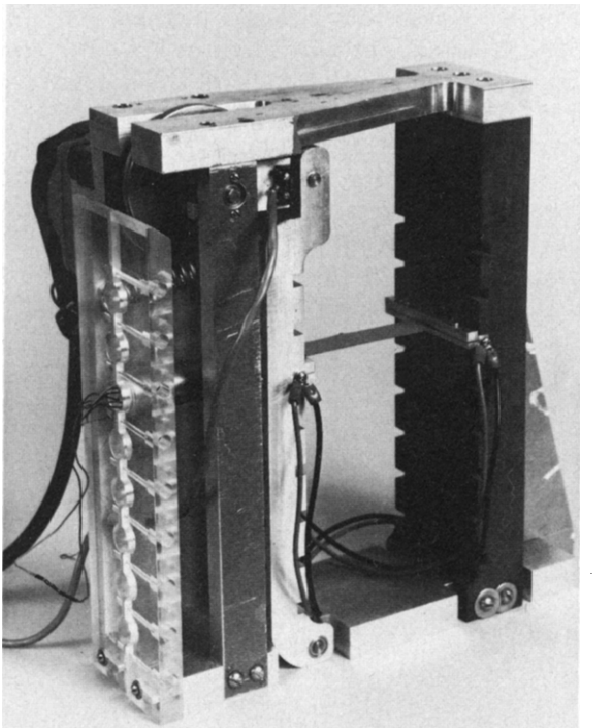

Fig. 6. Plaque fatigue testing machine.

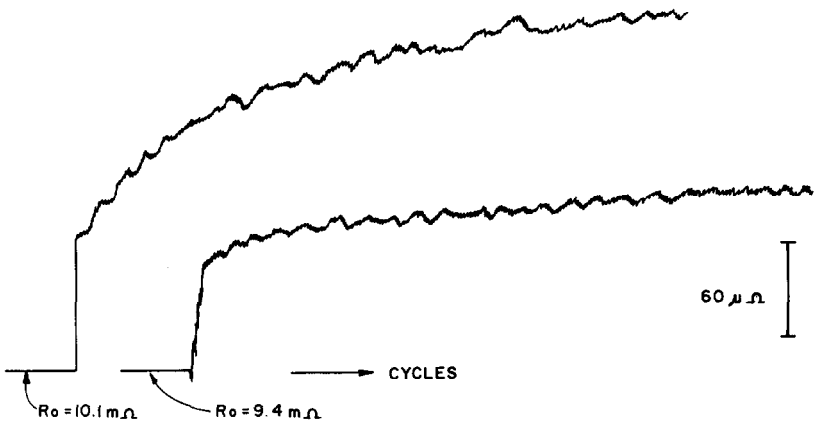

Fig. 7. 10 000 cycle fatigue test.

were taken from two different manufacturing lots. A manufacturing lot, in the sense of this paper, is a separate production run of material and is so designated by the manufacturer by an identifying lot number. The test conditions were a prestrain of 3.4×10^{-3} mm/mm and a cyclic strain of 8.5×10^{-4} mm/mm. These conditions were arrived at by testing four different manufacturing lots of plaque at various prestrains and cyclic strains for 1000

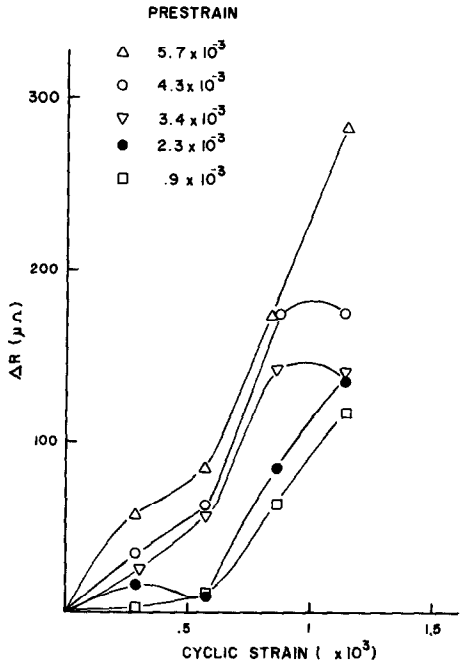

Fig. 8. Characteristic change in resistance, ΔR, for 1,000 cycle fatigue tests.

cycles per sample. The resistance change for each lot was plotted as shown in Fig. 8. Data for the other three lots are similar and are not presented here. The test conditions were chosen because of the consistency of the data obtained for each lot and the comparability to the actual strains observed (Figs. 3 - 5, and Table 1).

To compare the lot to lot fatigue characteristics, ten samples from each of the four lots were cycled 1000 times and the data statistically reduced. The resistance change, ΔR, of each sample was nondimensionalized by its initial resistance value, R. The results are shown in Table 2. Note that there are significant differences in the degree of plaque breakup ($\Delta R/R$) and thus different capacity retention characteristics of the plaque when considering long cycle lives.

TABLE 2

Fatigue characteristics of various plaque lots

Lot no.	1	2	3	4
Mean $\Delta R/R\left(\frac{\mu\Omega}{m\Omega} \times 10^3\right)$	12.00	12.17	18.54	19.43
Std. deviation of $\Delta R/R$	1.71	1.58	5.66	4.45

Hardness testing of plaque

The hardness test devised is of the indentation type. A ball is pressed into the plaque surface by a fixed load and the depression depth is used as an indication of the hardness.

The hardness test uses a 12.7 mm (0.500 in.) ball which is pressed into the surface initially by a 100 g tare weight (0 indentation reference) followed by a 400 g test weight. The indentation depth is measured by an LVDT.

In Fig. 9, an indentation *vs.* load curve is shown for plaque samples from a single lot. From this curve, the 100 g tare and 400 g test weights were chosen.

The hardness, H, of a sample is defined as follows:

$$H \equiv 1/\delta$$

where δ is the indentation due to the test load expressed in millimeters.

The importance of the hardness measurement is based upon previous data, Figs. 3 - 5, plus two experimental observations, one quantitative, the other qualitative. The quantitative results are shown in Fig. 10, utilization efficiency *vs.* hardness. These results were obtained by cycling each nickel electrode in a Ni/Cd test cell until the maximum utilization was observed (80 cycles or greater). The cell was discharged to 0.4 V on each cycle and a Cd third electrode was used to ensure that the cell remained nickel limited. The maximum utilization is interpreted in this Figure to represent the best electrochemical performance of which the test electrodes are capable. With this interpretation, it is concluded from Fig. 10, that the harder plaque limits the electrode performance. The variation in utilization efficiency for a given plaque hardness is a correct result and is associated with $Ni(OH)_2$ structural differences. These differences will be the subject of a future communucation. Similar utilization efficiency variation has been reported by Puglisi [6].

The qualitative experimental observation made is that the harder the plaque, the greater the shedding of active material. A hard plaque will tend to exude finely divided, black, active material which is readily seen to fall to the bottom of the test cell. A soft plaque will show little or no tendency to shed active material.

From the above observations, plus the previous data that harder plaque is subject to greater strains, and from the s.e.m. of nickel sinter, Fig. 11, the following heuristic argument on the significance of plaque hardness can be made.

Note from Fig. 11 that the nickel sinter does not appear to be a pore type structure, but rather a series of nickel "chains" that are free standing, interconnected, or terminated in agglomerate particles. The structure can therefore be viewed as agglomerate particles held together by chains. Thus, a hard plaque would have a rigid chain structure that does not allow the agglomerates to move significantly under the hardness test load.

In the active electrode, the sinter is covered with material that undergoes volumetric changes as it is charged and discharged [7]. These volumetric

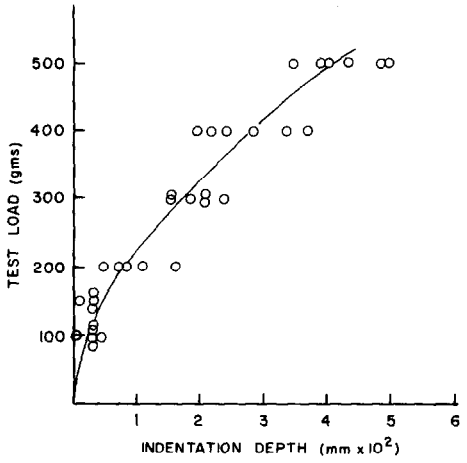

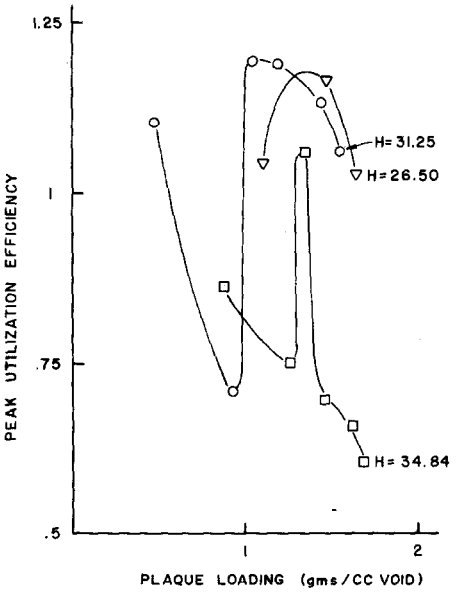

Fig. 9. Indentation into nickel plaque by 1.27 cm ball for various test loads.

Fig. 10. Utilization efficiency and the effect of plaque hardness.

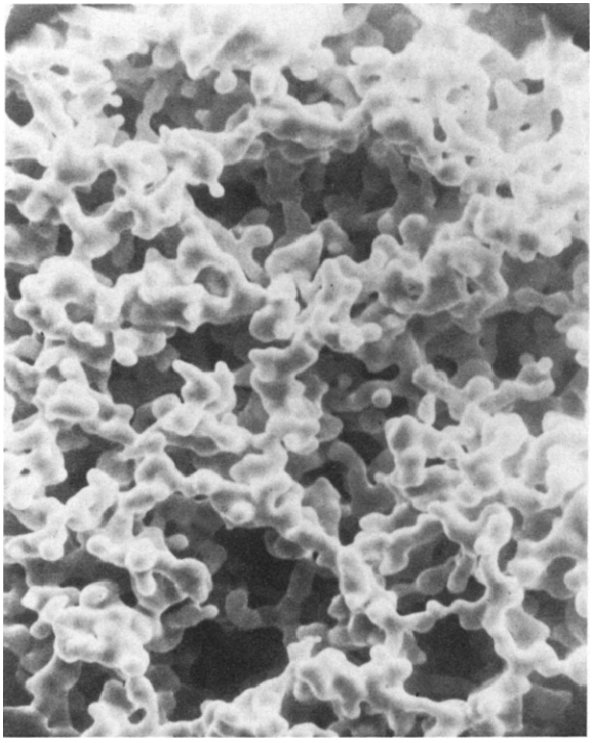

Fig. 11. Scanning electron micrograph of nickel sinter.

changes will cause deformation of the sinter chains, analogous to a bimetallic thermostat. In hard plaque, the more rigid chains will resist the deformation, thus not allowing full volumetric expansion of the active material and therefore limiting the utilization efficiency that can be obtained. Similarly, a given volumetric expansion of the active material implies a certain deformation of the chains. Thus, the more rigid chains of hard plaque will cause greater electrode distortion (growth) than soft plaque for a given value of A h/cc void. This is consistent with the results of Figs. 3 - 5.

The final observation, electrode shedding, is also consistent with this model. The deformation at the sinter chains is the result of the shear stresses at the interface between the active material and the sinter. To deform a comparatively rigid substrate *vs.* a soft one requires higher stress levels. Thus, a given A h/cm^3 void discharge implies higher stresses for hard plaque than for soft plaque. High interface stresses will result in the shedding of active material. This was amply demonstrated by McArthur [8] when he deposited $Ni(OH)_2$ on 0.127 mm thick nickel foils. The foil is a very rigid substrate and McArthur got very short cycle life due to active material shedding.

From the above discussion , it is concluded that plaque hardness is a very important parameter that affects both utilization efficiency and short term capacity retention *via* material shedding.

The relationship between the fatigue and hardness tests

Of concern when developing test procedures is that the tests devised are not interdependent. A strong interrelation would eliminate the need for all but one test. A casual inspection of the fatigue *vs.* hardness results would indicate that the tests are essentially unrelated. That is, good fatigue results have been obtained with both hard and soft plaque. However, there is a trend for hard plaque to be better in fatigue than soft plaque. It is important to know if these are real effects or random results.

To analyze the possible dependence, the model shown in Fig. 12 is used. G_s is the nonfatiguing portion of the plaque in the region of the current collector (a nickel screen collector). R_n is the resistance of the sinter between fatigue cracks. The conductance of the test sample is given by:

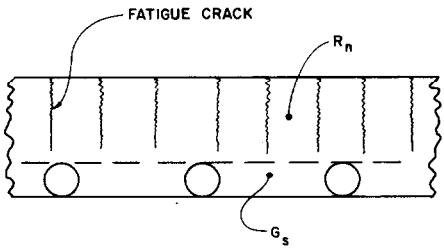

Fig. 12. Model of plaque used in sinter conductivity analysis.

$$G = G_s + \frac{1}{\sum_{1}^{n+1} R_n + n\left(\frac{1}{(m_s)(g_s) + (m_m)(g_m)}\right)} \tag{1}$$

where n is the number of fatigue cracks, g_s the conductivity of sinter connection, g_m the conductivity of broken sinter connections making mechanical contact, m_s the number of sinter connections at the fatigue crack, and m_m is the number of mechanical connections.

$$m = m_s + m_m. \tag{2}$$

The initial conductivity, G_o, is obtained by setting $m_m = 0$, *i.e.*, a broken sinter connection always makes mechanical contact. This is a reasonable assumption provided the yield point of the sinter is not exceeded. This appears to be true, as all the fatigue samples tested curl away from the current collector, indicating that the collector yields but the sinter does not. Proceeding with the analysis, eqn. (1) is differentiated with respect to cycles, c, and substitutions made for m_m and G_o to obtain

$$\frac{dG}{dc} = \frac{n(g_s)\left(1 - \frac{g_m}{g_s}\right)\frac{d(m_s)}{dc}}{\left[\left(\frac{1}{G_o - G_s}\right) m(g_s)\left(1 - \frac{(M_m)}{m} + \frac{(M_m)}{m}\frac{(g_m)}{(g_s)}\right) + n\frac{(M_m)}{m}\left(1 - \frac{(g_m)}{(g_s)}\right)\right]^2}$$

It is seen that the apparent rate of plaque breakup, dG/dc, is dependent on $(1 - g_m/g_s)$. If g_m/g_s approaches one, the test becomes insensitive to fatigue. Also if g_m/g_s is a function of H, the fatigue and hardness test are not independent. It thus is important to determine g_m/g_s. This is done by "cracking" the plaque to break the sinter connections and then restoring the crack to make mechanical connections. In Fig. 13, a diagram of the process is shown.

The following are expressions that give the test sample resistance as a function of the number of fractures

$$R_o = R_o$$

$$R_1 = R_o + \delta x/LR_s - \delta x/LR_o$$

$$R_2 = R_o + 2\delta x/LR_s - 2\delta x/LR_o$$

.

.

.

$$R_n = R_o + n\delta x/L(R_s - R_o)$$

.

.

$$RN = R_s$$

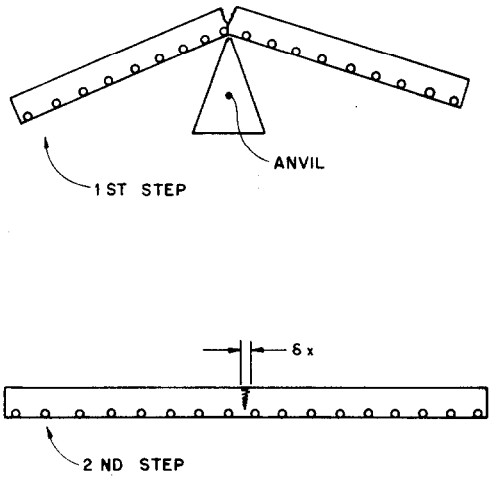

Fig. 13. Procedure for determining g_m/g_s.

where R_o is the resistance of the unbroken sample, R_s the resistance of the nonfractured current collector zone, L the sample length, δx the fracture zone length, n the number of fractures, and $N = L/\delta x$ is the maximum number of fractures.

Consider the following sequence:

(1) measure R_o;

(2) fracture sample and measure R_1;

(3) fatigue sample in bending over 25.4 mm arbor and measure RN (see ref. 2).

From the expression for R_1 and RN one obtains

$$\frac{\delta x}{L} = \frac{R_1 - R_o}{RN - R_o}. \tag{3}$$

Now $\delta x/L$ can be written as

$$\frac{\delta x}{L} R_o = \frac{1}{m(g_s) + \dfrac{1}{\dfrac{\delta x}{L} R_s}} \tag{4}$$

and if the single fracture is restored, as shown in Fig. 13, the test sample resistance, R, becomes

$$R = R_o - \frac{\delta x}{L} R_o + \frac{1}{m(g_m) + \dfrac{1}{\dfrac{\delta x}{L} R_s}}. \tag{5}$$

TABLE 3

Results of the fracture test sequence

H	$R_o/m\Omega$	$R_1 - R_o/\mu\Omega$	$R - R_o/\mu\Omega$	$R_s/m\Omega$	N/M
18.6	10.4	44	34	12.8	55/60
20.3	10.8	43	34	12.8	47/74
21.3	9.9	34	28	11.9	59/68
24.6	9.9	42	30	12.2	55/69
20.0	11.1	42	35	12.6	35/65
20.6	10.8	28	23	12.1	46/81
26.3	9.5	42	29	11.9	57/57
26.3	9.4	34	20	11.5	62/60

In Table 3, the results of the above fracture sequence are shown.

The N/M column in Table 3 is the ratio of the calculated fractures from eqn. (3) to the actual counted fractures, M, from bending over the 25.4 mm arbor. This ratio is an indication of the validity of the analysis technique. In general, the results are very satisfactory, which suggests that the analysis is essentially correct.

From eqns. (3) - (5), g_m/g_s is calculated. In Fig. 14, the dependence of g_m/g_s on H is shown. This Figure shows that $g_m/g_s \ll 1$ and therefore the fatigue test used is sensitive to the breaking of sinter joints; secondly, there is some interdependence between the hardness and fatigue tests. Thus, hard plaque will tend to give artifically high fatigue life when compared with soft plaque.

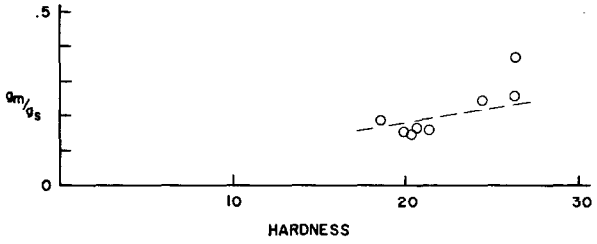

Fig. 14. Mechanical to sinter connection conductivity ratio *vs.* plaque hardness.

Conclusions

The emphasis of this work has been on the mechanical characteristics of sintered nickel plaque, and how these characteristics relate to known failure mechanisms and performance limitations of $Ni(OH)_2$ electrodes. It has been found that the "usual" quality control procedures applied to plaque are not entirely adequate.

One of the necessary additional tests is to measure the fatigue life of the plaque in order to ensure good, long term capacity retention characteristics. For the $Ni(OH)_2$ impregnation process used in this work, it was found that a prestrain of 3.4×10^{-3} plus a cyclic strain of 8.5×10^{-4} simulated the strains observed in a cell. In addition, it was found that various seemingly identical manufacturing lots of plaque showed a marked variation in their fatigue life when subjected mechanically to the above strains.

Another important test is the nickel sinter hardness. A "soft" sinter is generally desirable from the viewpoint of obtaining good utilization efficiency and avoiding the shedding of active material. It was found that hardness tests and fatigue tests are essentially independent test techniques. In addition, a "soft" sinter does not imply poor fatigue characteristics.

Acknowledgements

The author thanks the Air Force Scientific Research for partial financial support of this work. Additionally, he is indebted to Mr. John Leonard for his valuable experimental assistance and to Mr. Don Warnock for his helpful discussions.

References

1 T. Katan and H. F. Bauman, *J. Electrochem. Soc., 122* (1975) 77.
2 H. N. Seiger, V. J. Puglisi, P. F. Ritterman and D. F. Pickett, *Proc. 9th IECEC Meeting, 1974.*
3 D. H. Fritts, *AFAPL-TR-78-37,* 1978.
4 D. H. Fritts, in J. Thompson (ed.), *Power Sources 7,* Academic Press, New York, 1979, Ch. 7.
5 D. F. Pickett, *U. S. Patent 3,827,911, (1974).*
6 V. J. Puglisi, Development of nickel-oxide electrodes for use in nickel–hydrogen cells, *Proc. 1976 Goddard Space Flight Center Battery Workshop, November, 1976.*
7 P. P. McDermott, Failure analysis of cells in an accelerated test program, Coppin State College.
8 D. M. McArthur, in D. H. Collins (ed.), *Power Sources 3,* Oriel Press, Newcastle upon Tyne, 1971, Ch. 6.